Supplementary material

Regulating interfacial polymerization via multi-functional calcium carbonate based interlayer for highly permselective nanofiltration membrane

Mengyang Hu[a], Wenming Fu[a,b], Kecheng Guan[a], Ralph Rolly Gonzales[a], Qiangqiang Song[a,b], Atsushi Matsuoka[a,b], Zhaohuan Mai[a], Yu-Hsuan Chiao[a], Pengfei Zhang[a], Zhan Li[a], Hideto Matsuyama[a,b]*

[a] Research Center for Membrane and Film Technology, Kobe University, 1-1 Rokkodaicho, Nada, Kobe, 657-8501, Japan

[b] Department of Chemical Science and Engineering, Kobe University, 1-1 Rokkodaicho, Nada, Kobe, 657-8501, Japan

∗ Corresponding author.

E-mail: matuyama@kobe-u.ac.jp (H. Matsuyama).

Reaction heat measurement

In this system, the temperature of a reactor was adjusted by controlling the temperature of a jacket. The method to measure the heat of the reaction is described below. 60 mL of 0.2 wt.% PIP aqueous solution (PIP system) or 60 mL of 0.2 wt.% PIP aqueous solution with $CaCO_3$ nanoparticles (PIP-$CaCO_3$ system) was added to the reactor. The $CaCO_3$ nanoparticles were prepared by mixing 0.05 M $CaCl_2$ aqueous solution and 0.02 M Na_2CO_3 aqueous solution. Then the temperature of the system was adjusted to 298 K with stirred at 200 rpm. After the stabilization for 60 min, 10 mL of 0.1 wt.% TMC/hexane solution was drop wisely added to the reactor.

During the reaction, the temperature of the reactor, T_R (K), and the jacket, T_J (K), was monitored. The total heat generated by the reaction is equal to the total heat that was transferred from the reactor to the jacket during the reaction. The rate of heat transfer from the reactor to the jacket, Q (J s^{-1}) is expressed as the following equation:

$$Q = U \cdot A(T_R - T_J)$$

where, U (J m^{-2} K^{-1} s^{-1}) and A (m^2) are heat transfer coefficient and surface area, respectively. Therefore, the heat of the reaction, H (J), could be calculated by the integration of Q during the reaction time.

$$H = \int U \cdot A(T_R - T_J)$$

The value of UA was determined by calibration as 625.9×10^{-3} J K^{-1} s^{-1}.

The characterization of $CaCO_3$ nanoparticles size on PK-6 membrane surface

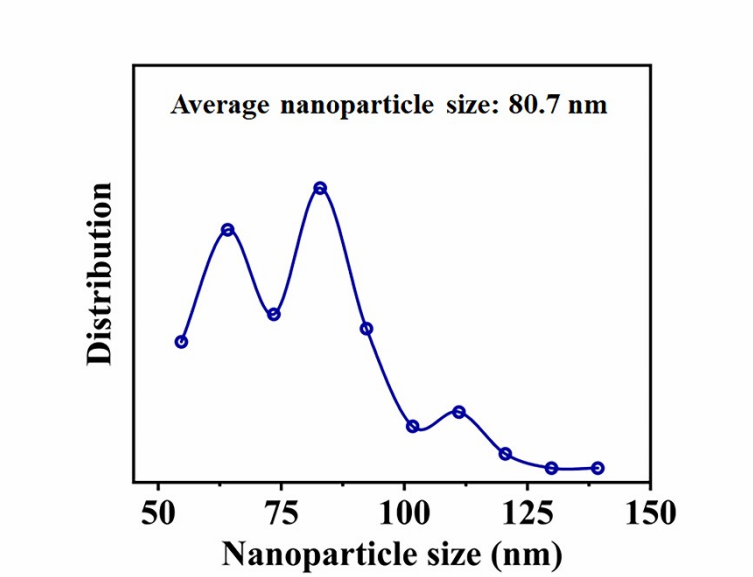

Fig. S1. Statistics of $CaCO_3$ nanoparticle size distribution.

The $CaCO_3$ nanoparticles size on PK-6 membrane surface were used to analyze by Nano Measurer software.

The surface and overall pore size/porosity of PK support membranes

Table S1. The changes in the surface and overall pore size/porosity of PK supports as a function of LbL cycles.

Membranes	Surface pore size (nm)	Surface porosity (%)	Overall porosity (%)
PK-0	181.9±21	31.2±2	76.1±3
PK-4	168.2±18	28.8±1	74.9±2
PK-5	135.3±16	24.7±3	72.8±3
PK-6	122.5±13	22.3±1	73.5±4
PK-7	107.2±15	18.6±2	71.3±2

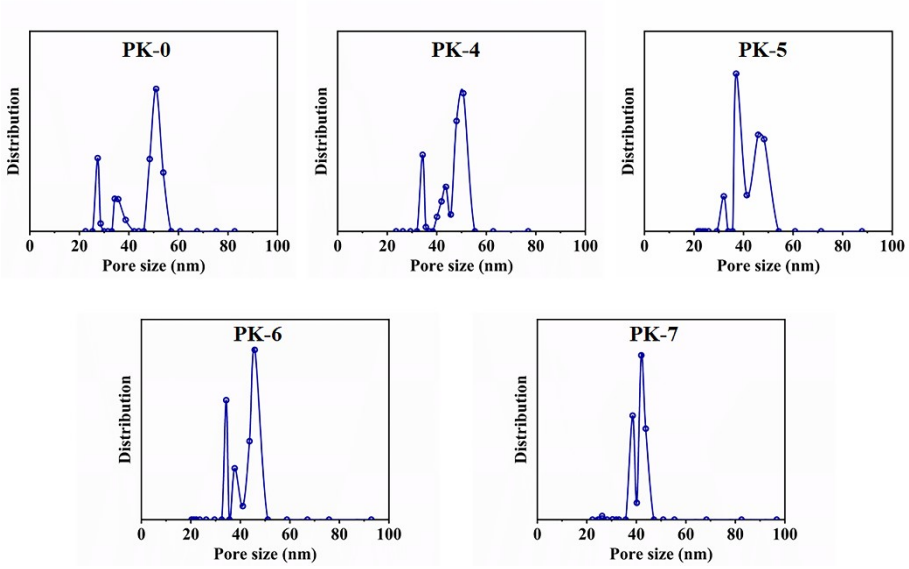

Fig. S2. Overall pore size distributions of membranes.

The membranes surface pore size and surface porosity were used to analyze by Nano Measurer software and ImageJ software, respectively. The membranes overall porosity were determined by gravimetric method.[1] The overall pore size and pore size distribution of the membranes were assessed using liquid-liquid porometer (LLP-1200A, Porous Materials Inc., NY, USA). Fig. S2 showed the average overall pore size of PK-0, PK-4, PK-5, PK-6 and PK-7 membranes were 50.3 nm, 48.6 nm, 44.2 nm, 43.3 nm and 41.8 nm, respectively.

Distributions of Ca element on the PK-6 surface

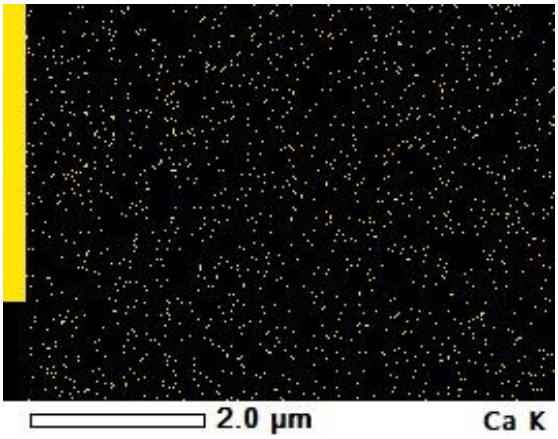

Fig. S3 Distributions of Ca element (points measured by EDX mapping analysis) on the PK-6 surface.

The cross-sectional EDX images of PK-6 membrane

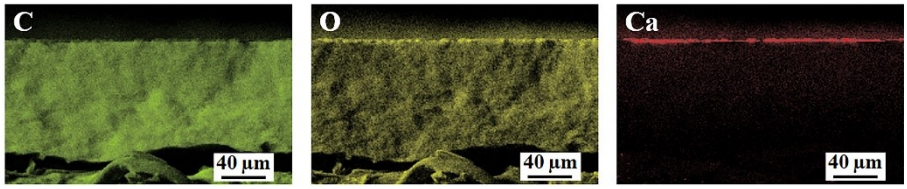

Fig. S4. The cross-sectional EDX images of PK-6 membrane.

Crosslinking degree of membranes

The crosslinking degree of the membrane could be evaluated by calculating the atomic concentration of each element at the membrane surface using the following equations[2]

$$Crosslinking\ degree\ (\%) = \frac{m}{m+n} \times 100 \quad (1)$$

where the values of m and n are derived from the experimental O/N ratio according to the XPS characterization results using Eqs. (2) and (3), respectively:

$$m + n = 1 \quad (2)$$

$$\frac{O}{N} = \frac{3m + 4n}{3m + 2n} \quad (3)$$

Table S2. Elemental composition and crosslinking degree of NF membranes

Membranes	Atomic concentration (%)			Crosslinking degree (%)
	C (1s)	O (1s)	N (1s)	
PK-NF-0	64.79	19.16	16.05	73.5
PK-NF-4	62.55	20.73	16.72	67.9
PK-NF-5	62.06	21.16	16.78	65.4
PK-NF-6	60.47	22.28	17.25	61.8
PK-NF-7	60.51	22.63	16.86	56.2

Data of reaction heat measurement

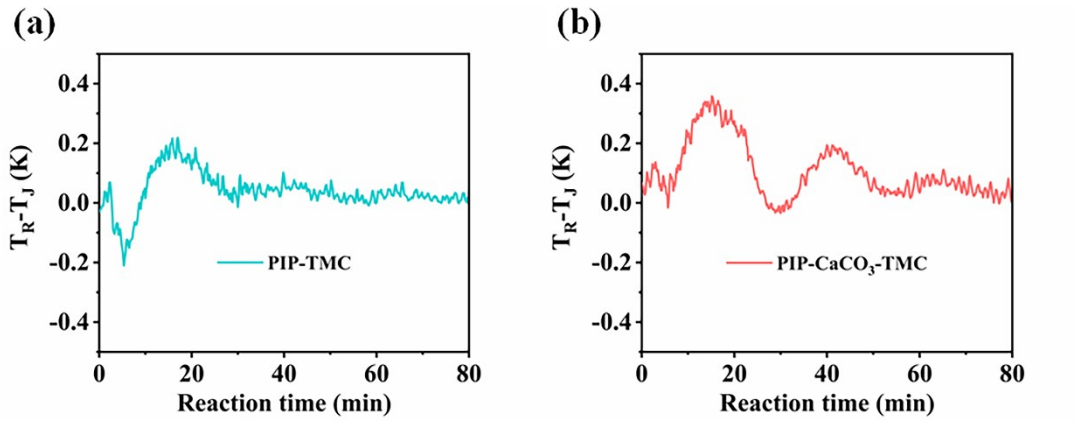

Fig. S5 Temperature difference between the reactor and jacket as a function of reaction time (a) PIP-TMC system; (b) PIP-$CaCO_3$-TMC system.

The characterization of TA-coated PK support/NF membranes

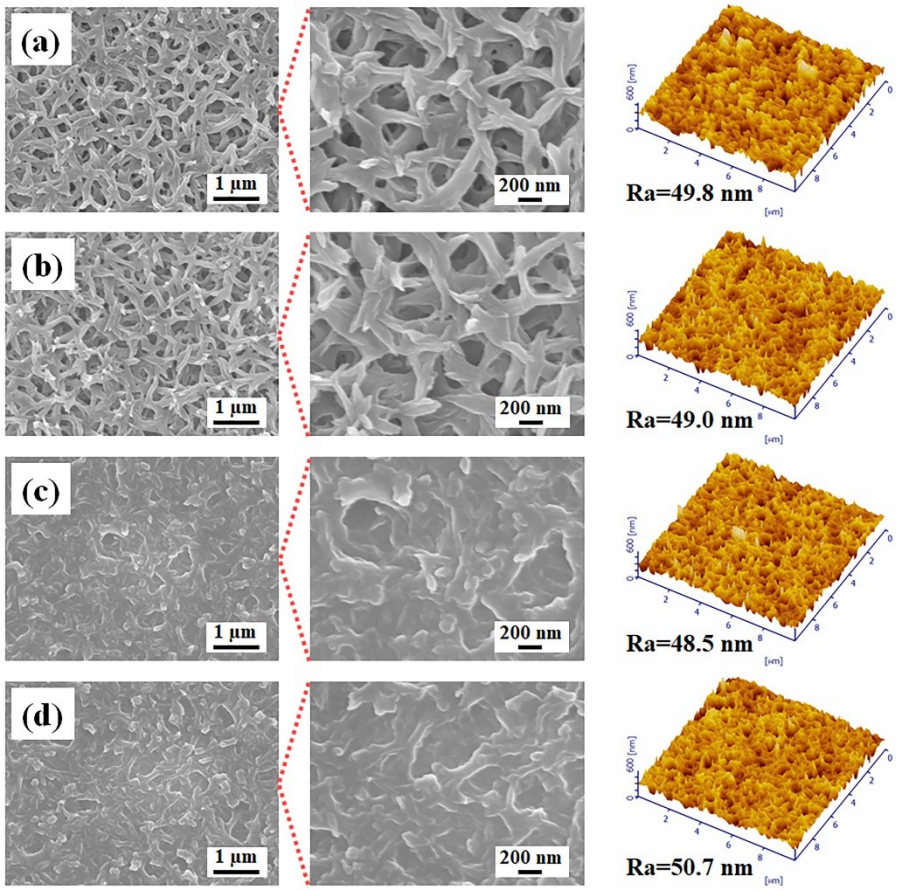

Fig. S6 Surface SEM and AFM images of membranes: (a) PK/TA-12h support membrane; (b) PK/TA-24h support membrane; (c) PK/TA-12h-NF membrane; (d) PK/TA-24h-NF membrane.

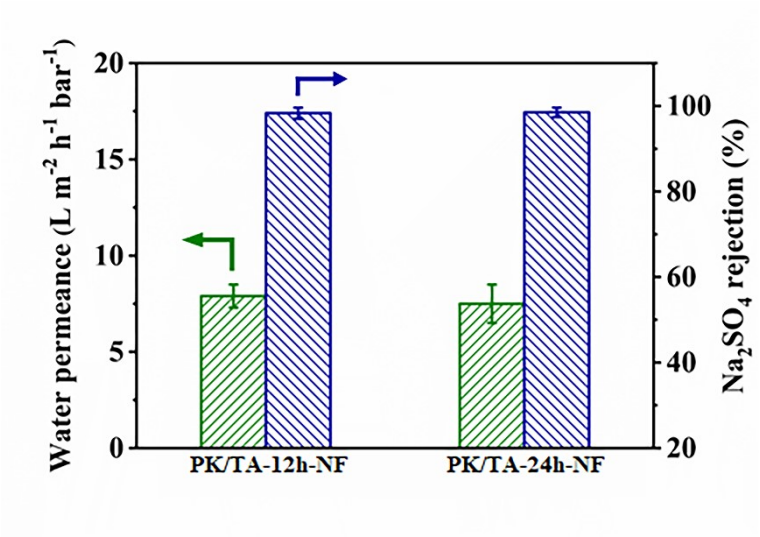

Fig. S7 The pure water permeance and Na_2SO_4 rejection of NF membranes.

In order to prepare support membranes with different TA coating times, the PK membranes were soaked into TA aqueous solution (0.1 wt.%) for 12 h and 24 h, respectively. Afterwards, the membranes were washed with water, and finally dried in the air. The resultant membranes were designated as PK/TA-12h and PK/TA-24h, respectively. Following similar procedures, the NF membranes were fabricated by using TA-coated PK membrane as the porous support. The obtained membranes with various TA coating times were denoted as PK/TA-12h-NF and PK/TA-24h-NF, respectively. It can be seen from Fig. S6 that the TA-coated PK support/NF membranes possessed a similar surface morphologies and average roughness values with the pristine PK support/NF membranes. Meanwhile, the water permeance of PK/TA-12h-NF membranes and PK/TA-24h-NF membranes is 7.9 L m^{-2} h^{-1} bar^{-1} and 7.5 L m^{-2} h^{-1} bar^{-1}, respectively (Fig. S7).

Various salts rejection of the PK-NF-0 membrane

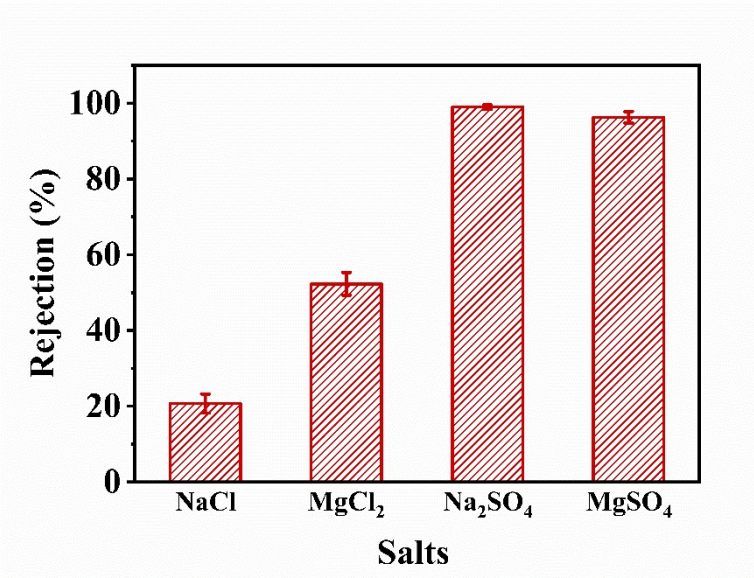

Fig. S8 Salts rejection of the PK-NF-0 membrane.

The salt rejection for PK-NF-0 membrane follow a sequence of Na_2SO_4 (99.0%) > $MgSO_4$ (96.3%) > $MgCl_2$ (52.3%) > NaCl (20.7%), which is a typical PIP-based NF desalination performance depend on the synergy of size sieving and Donnan effect.[3] This can be illustrated as: (1) The PK-NF-0 membrane with a negative surface charge (Fig. 7 (d)) prefers to reject divalent anions rather than divalent cations and (2) the hydrated ion radius of Na^+ (0.358 nm) and Cl^- (0.332 nm), which are smaller than those of SO_4^{2-} (0.379 nm) and Mg^{2+} (0.428 nm).[4]

pH stability test of PK-NF-6 membrane

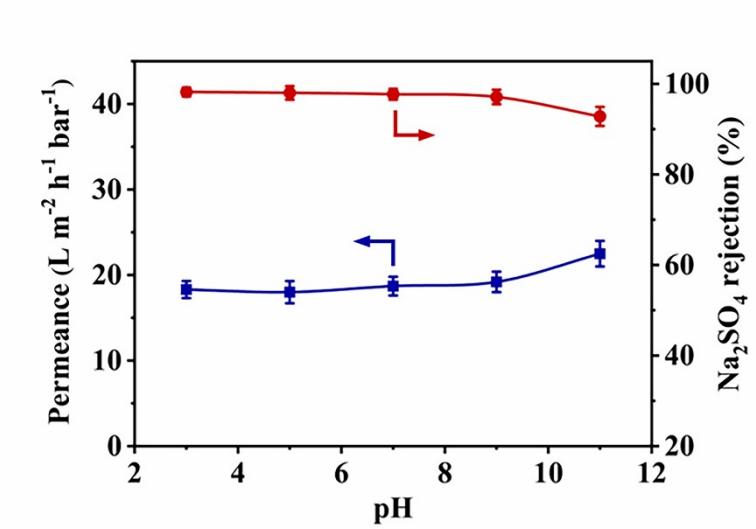

Fig. S9. The permeance and Na_2SO_4 rejection of PK-NF-6 membrane after filtration with the aqueous solution for 2 h under different pH.

In order to evaluate the pH stability of PK-NF-6 membrane, the membrane was first filtered with the aqueous solution for 2 h under different pH conditions (pH=3, 5, 7, 9 and 11). And then, the permeance and Na_2SO_4 rejection of the membrane were tested under 0.5 MPa. The pH was adjusted by the addition of small amount of HCl and NaOH for deionized water respectively. It can be observed from Fig. S9 that the permeance and Na_2SO_4 rejection of PK-NF-6 membrane maintained steady after filtration with the aqueous solution for 2 h under pH=3, 5, 7 and 9. In addition, the permeance increased from 18.7 L m^{-2} h^{-1} bar^{-1} to 22.5 L m^{-2} h^{-1} bar^{-1} and the Na_2SO_4 rejection reduced from 97.7 % to 92.8 % after filtration with the aqueous solution for 2 h from pH=7 to pH=11. This is because of the partial hydrolyzation of ester bonds/amide bonds, which could increase the free volume of the cross-linked structure

in the selective layer.[5]

NF performance comparison between PK-NF-6 membrane and membranes in literature

Table S3. Comparison of NF performance of PK-NF-6 membrane with other membranes in literature.

Membranes	Operation pressure (MPa)	Pure water permeance (L m^{-2} h^{-1} bar^{-1})	Na_2SO_4 rejection (%)	Ref.
(PIP+SDS)-TMC	0.4	17.1	99.6	[2]
Co-7:3@PA	1.0	15.7	98.3	[6]
GE-Osmonics DL	3.0	10.0	96.0	[7]
NF-270	1.0	11.6	94.0	[8]
PA50/CNC/PES	0.6	34.0	96.7	[9]
PA-Co-3.0/PSf	1.0	20.4	96.8	[10]
PA-SiO_2-4h/PSf	1.0	14.5	98.7	[11]
PD/SWCNTs/NF	0.6	32.0	95.9	[12]
PIP-TMC (EIP)	0.5	16.6	95.5	[13]
TFC2.0-5	0.4	14.5	97.0	[14]
TFC-CNT-2	0.5	21.0	98.3	[15]

TFN-CN/HNT	0.4	20.5	94.5	[16]
TFNM-HZN$_{CS}$	0.6	12.2	94.7	[17]
TFN-PDA-SiNPs	0.6	13.3	97.0	[18]
TFN-PDP	0.6	9.9	98.0	[19]
Vacuum-PA	0.6	20.0	99.6	[20]
PK-NF-6	0.5	23.4	97.7	This work

References

1. L. Zhang, Z. Cui, M. Hu, Y. Mo, S. Li, B. He, J. Li, J. Membr. Sci. 2017, 540, 136-145.
2. Y. Liang, Y. Zhu, C. Liu, K. R. Lee, W. S. Hung, Z. Wang, Y. Li, M. Elimelech, J. Jin, S. Lin, Nat. Commun. 2020, 11, 2015.
3. J. Zhu, J. Hou, R. Zhang, S. Yuan, J. Li, M. Tian, P. Wang, Y. Zhang, A. Volodin, B. Van der Bruggen, J. Mater. Chem. A. 2018, 6, 15701-15709.
4. M.-Q. Ma, C. Zhang, C.-Y. Zhu, S. Huang, J. Yang, Z.-K. Xu, J. Membr. Sci. 2019, 591, 117316.
5. J. Tian, B. Song, S. Gao, B. Van der Bruggen, R. Zhang, J. Membr. Sci. 2022, 642, 119984.
6. Y. Lin, X. Yao, Q. Shen, T. Ueda, Y. Kawabata, J. Segawa, K. Guan, T. Istirokhatun, Q. Song, T. Yoshioka, H. Matsuyama, Nano. Lett, 2021, 21, 6525-6532.
7. Y.-J. Tang, Z.-L. Xu, S.-M. Xue, Y.-M. Wei, H. Yang, J. Membr. Sci. 2016, 498, 374-384.
8. F. Peng, X. Huang, A. Jawor, E. M. V. Hoek, J. Membr. Sci. 2010, 353, 169-176.
9. J.-J. Wang, H.-C. Yang, M.-B. Wu, X. Zhang, Z.-K. Xu, J. Mater. Chem. A. 2017, 5, 16289-16295.
10. Q. Song, Y. Lin, T. Ueda, Q. Shen, K.-R. Lee, T. Yoshioka, H. Matsuyama, J. Membr. Sci. 2022, 657, 120679.
11. Q. Song, Y. Lin, T. Ueda, T. Istirokhatun, Q. Shen, K. Guan, T. Yoshioka, H.

Matsuyama, J. Mater. Chem. A. 2021, 9, 26159-26171.

12. Y. Zhu, W. Xie, S. Gao, F. Zhang, W. Zhang, Z. Liu, J. Jin, Small. 2016, 12, 5034-5041.
13. S. Yang, J. Wang, L. Fang, H. Lin, F. Liu, C.Y. Tang, J. Membr. Sci. 2020, 602, 117971.
14. J. Zhu, S. Yuan, A. Uliana, J. Hou, J. Li, X. Li, M. Tian, Y. Chen, A. Volodin, B.V. der Bruggen, J. Membr. Sci. 2018, 554, 97-108.
15. G. Gong, P. Wang, Z. Zhou, Y. Hu, ACS Appl. Mater. Inter. 2019, 11, 7349-7356.
16. Y. Liu, X. Wang, X. Gao, J. Zheng, J. Wang, A. Volodin, Y.F. Xie, X. Huang, B. Van der Bruggen, J. Zhu, J. Membr. Sci. 2020, 596, 117717.
17. Z. Sun, Q. Wu, C. Ye, W. Wang, L. Zheng, F. Dong, Z. Yi, L. Xue, C. Gao, Nano. Lett, 2019, 19, 2953-2959.
18. M. B. M. Y. Ang, C. A. Trilles, M. R. De Guzman, J. M. Pereira, R. R. Aquino, S.-H. Huang, C.-C. Hu, K.-R. Lee, J.-Y. Lai, Sep. Purif. Technol. 2019, 224, 113-120.
19. M. B. M. Y. Ang, Y.-L. Ji, S.-H. Huang, K.-R. Lee, J.-Y. Lai, J. Membr. Sci. 2019, 579, 79-89.
20. C.-Y. Zhu, H.-N. Li, J. Yang, J.-J. Li, J.-R. Ye, Z.-K. Xu, J. Membr. Sci. 2020, 616, 118557.